A new set of standards for in-situ measurement of bromine abundances in natural silicate glasses: application to SR-XRF, LA-ICP-MS and SIMS techniques

Anita Cadoux, Giada Iacono-Marziano, Antonio Paonita, Etienne Deloule, A. Aiuppa, Nelson G. Eby, Michela Costa, Lorenzo Brusca, Kim Berlo, Kalotina Geraki, et al.

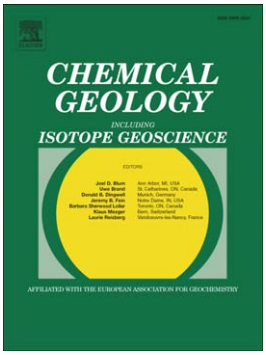

A new set of standards for *in-situ* measurement of bromine abundances in natural silicate glasses: application to SR-XRF, LA-ICP-MS and SIMS techniques

Anita Cadoux, Giada Iacono-Marziano, Antonio Paonita, Etienne Deloule, Alessandro Aiuppa, G. Nelson Eby, Michela Costa, Lorenzo Brusca, Kim Berlo, Kalotina Geraki, Tamsin A. Mather, David M. Pyle, Ida Di Carlo

PII: S0009-2541(17)30026-8
DOI: doi:10.1016/j.chemgeo.2017.01.012
Reference: CHEMGE 18224

To appear in: *Chemical Geology*

Received date: 30 August 2016
Revised date: 12 January 2017
Accepted date: 16 January 2017

Please cite this article as: Cadoux, Anita, Iacono-Marziano, Giada, Paonita, Antonio, Deloule, Etienne, Aiuppa, Alessandro, Nelson Eby, G., Costa, Michela, Brusca, Lorenzo, Berlo, Kim, Geraki, Kalotina, Mather, Tamsin A., Pyle, David M., Di Carlo, Ida, A new set of standards for *in-situ* measurement of bromine abundances in natural silicate glasses: application to SR-XRF, LA-ICP-MS and SIMS techniques, *Chemical Geology* (2017), doi:10.1016/j.chemgeo.2017.01.012

A new set of standards for *in-situ* measurement of bromine abundances in natural silicate glasses: application to SR-XRF, LA-ICP-MS and SIMS techniques

Anita Cadoux [a,b,c*], Giada Iacono-Marziano [a,b,c], Antonio Paonita [d], Etienne Deloule [e], Alessandro Aiuppa [d,f], G. Nelson Eby [g], Michela Costa [f], Lorenzo Brusca [d], Kim Berlo [h], Kalotina Geraki [i], Tamsin A. Mather [j], David M. Pyle [j], Ida Di Carlo [a,b,c]

[a] Université d'Orléans, ISTO, UMR 7327, 45071, Orléans, France

[b] CNRS, ISTO, UMR 7327, 45071 Orléans, France

[c] BRGM, ISTO, UMR 7327, BP 36009, 45060 Orléans, France

[d] Istituto Nazionale di Geofisica e Vulcanologia, Sezione di Palermo, Italy

[e] CNRS, CRPG, UMR 7358, Université de Lorraine, BP 20, 54501 Vandoeuvre-lès-Nancy Cedex, France

[f] DiSTeM, Università di Palermo, Italy

[g] Department of Environmental, Earth, & Atmospheric Sciences, University of Massachusetts, Lowell, MA 01854, USA

[h] Department of Earth and Planetary Sciences, McGill University, Montreal H3A 0E8, Canada

[i] Diamond Light Source, Harwell Science and Innovation Campus, Didcot OX11 0DE, UK

[j] Department of Earth Sciences, University of Oxford, Oxford OX1 3AN, UK

* Corresponding author: Anita Cadoux

Institut des Sciences de la Terre d'Orléans
Université d'Orléans/CNRS
1A, rue de la Férollerie
45071 Orléans Cedex 2
France
E-mail: acadoux@cnrs-orleans.fr

Abstract

Measuring the low bromine abundances in Earth's materials remains an important challenge in order to constrain the geodynamical cycle of this element. Suitable standard materials are therefore required to establish reliable analytical methods to quantify Br abundances. In this study we characterise 21 Br-doped glasses synthesized from natural volcanic rocks of mafic to silicic compositions, in order to produce a new set of standards for Br analyses using various techniques. The nominal Br contents (amounts of Br loaded in the experimental samples) of 15 of 21 glasses were confirmed within 20% by instrumental neutron activation analysis (INAA). Using this new set of standards, we compare three micro-analytical approaches to measure Br contents in silicate glasses: synchrotron X-ray fluorescence (SR-XRF), laser ablation-inductively coupled plasma mass spectrometry (LA-ICP-MS), and secondary ion mass spectrometry (SIMS). With SR-XRF, the Br contents of the standard glasses were determined with the highest accuracy (<10% for Br ≥ 10 ppm; > 25% for Br ≤ 5 ppm), and high precision (< 10% for Br contents > 10 ppm; 20-30% for Br ≤ 10 ppm). The detection limit was estimated to be less than 1 ppm Br. All those factors combined with a high spatial resolution (5x5 μm for the presented measurements), means that SR-XRF is well suited to determine the low Br abundance in natural volcanic glasses (crystal-hosted melt inclusions or matrix glasses of crystallized samples). At its current stage of development, the LA-ICP-MS method allows the measurement of hundreds to thousands ppm Br in silicate glasses with a precision and accuracy generally within 20 %. The Br detection limit of this method has not been estimated but its low spatial resolution (90 μm) currently prevents its use to characterise natural volcanic glasses, however it is fully appropriate to analyse super liquidus or sparsely phyric, Br-rich experimental charges. Our study shows that SIMS appears to be a promising technique to measure the low Br contents of natural volcanic glasses. Its spatial resolution is relatively good (~15 μm) and, similarly to SR-XRF, the detection limit is estimated to be ≤ 1 ppm. Using our new set of standards, the Br contents of two MPI-DING reference glasses containing less than 1.2 ppm of Br were reproduced with precision < 5% and accuracy < 20%. Moreover, SIMS presents the advantage of being a more accessible instrument than SR-XRF and data processing is more straightforward.

Keywords: bromine, volcanic glasses, INAA, SIMS, LA-ICP-MS, SR-XRF.

1. Introduction

Halogens are minor volatiles in the Earth's mantle and crust, but they have significant and specific influences on magmatic and degassing processes. Chlorine and fluorine behaviour in magmas are now relatively well constrained from several experimental studies (for a review, see Baker and Alletti, 2012). In contrast, bromine behaviour is much less known probably because Br concentrations in magmatic, mantle, or meteoritic samples are extremely low (ppb to < 300 ppm; Aiuppa et al., 2009; Pyle and Mather, 2009, and references therein), which makes accurate measurements more difficult. Despite its low abundance, Br may play a significant role in environmental processes. For example, Br has been recognized as an important component in volcanic gases (e.g., Bobrowski et al., 2003; Bureau et al., 2000; Gerlach, 2004; Oppenheimer et al., 2006; Theys et al., 2009) and it has been demonstrated that volcanogenic Br species are involved in the destruction of ozone (e.g., Cadoux et al., 2015; Kutterolf et al., 2013; Millard et al., 2006; Oppenheimer et al., 2010), being about 45 times more efficient than Cl in this respect (e.g., Daniel et al., 1999).

However, data required to quantify the global volcanic Br contribution to the atmosphere, and to constrain the Earth's bromine geodynamical cycle, are still scarce. In order to constrain the bromine cycle, we need to know the Br fluxes from Earth's deep mantle to the atmosphere, the Br flux back to the mantle through the subduction of oceanic crust, and the physical and chemical factors that affect the relative amounts of Br released to the atmosphere, retained in the upper mantle, or transferred to deeper reservoirs (e.g., Bureau et al., 2010). To answer these questions, establishing reliable analytical methods for determining Br abundances in geological materials remains an important challenge (e.g., Balcone et al., 2009; Boulyga and Heumann, 2005; Kendrick, 2012; Marks et al., 2012, 2016; Ruzié-Hamilton et al., 2016; Sekimoto and Ebihara, 2016; Seo et al., 2011).

Our study aimed to produce a set of standards to measure Br abundance in silicate glasses with micro-analytical techniques. We synthesized Br-doped hydrated glasses of mafic to silicic compositions from natural volcanic rocks, and determined their Br content using a bulk analytical technique: the instrumental neutron activation analysis (INAA). We then employed this set of standards to test the feasibility of Br analysis in silicate glasses by laser ablation-inductively coupled plasma mass spectrometry (LA-ICP-MS) and secondary ion mass spectrometry (SIMS). Bromine analyses were also performed with synchrotron X-ray fluorescence (SR-XRF), a technique that has already been used to analyze the low Br contents (generally ≤ 10 ppm) in natural volcanic glasses (e.g., Costa, 2014; Kutterolf et al., 2013;

Kutterolf et al., 2015). LA-ICP-MS and SIMS have been previously employed to analyze Br in minerals and fluid inclusions (Hammerli et al., 2013; Seo et al., 2011), and in apatite (Marks et al., 2012), respectively, but not in silicate glasses of natural composition. We therefore discuss the advantages and drawbacks of these three micro-analytical techniques and the applicability of LA-ICP-MS and SIMS to quantify Br contents in natural volcanic glasses.

2. Synthesis of Br-doped silicate glasses

2.1. Starting materials

The selected starting materials are natural volcanic rocks: a hawaiitic basalt from the 11/22/2002 Mt Etna eruption (also used by Lesne et al., 2011a, 2011b and by Iacono-Marziano et al., 2012), a calc-alkaline andesite from the Santorini Upper Scoria 2 (USC-2) eruption and a rhyodacite from the Santorini Minoan eruption (also used in Cadoux et al., 2014). Whole-rocks compositions are given in Table 1.

2.2. Preparation and experimental procedure

The whole-rocks were crushed and ground in an agate mortar. About 10 g of powder was melted twice (with quenching and grinding in between) in a platinum crucible placed in a piezoceramic oven at 1400°C - 1 atm for 3-4 hours, to ensure homogenization. The resulting dry glasses (Table 1) were then reduced to powder.

About 240-300 mg of glass powder was loaded into Pt or Au-Pd capsules (inner diameter 5.0 mm, outer diameter 5.4 mm, ~ 3 cm in length) together with known amounts of Br-bearing solutions (2 to 4 wt%) in order to synthesize a set of standards with a wide range of Br contents: 0.5 to 6,000 ppm for the basaltic composition, 10 to 5,000 ppm for the andesitic and rhyodacitic compositions. Br-bearing solutions with different concentrations were prepared by dissolving NaBr salt into distilled water. Using this technique the uncertainty in the Br content loaded into the capsule is reasonably low (between 1.9 and 5.5 % of the calculated value) and independent of Br concentration.

In order to limit the Au content of the melt, Pt capsules were generally preferred for synthesizing glasses with low Br contents. Indeed, Au raises background counts during INAA and therefore increases the Br detection limit for this technique. Pt has little effect as it does not activate the way Au does. After loading, the capsules were welded shut, weighed and dipped into hot oil to check for potential volatile leaks. They were stored in an oven at 120°C for a couple of hours and reweighed before the experiment.

The Br-doped glasses were synthesized at the Institut des Sciences de la Terre d'Orléans (ISTO, Orléans, France) in an internally heated pressure vessel (IHPV). Experiments were performed at temperatures of 1200-1250°C, pressures of 300-400 MPa and for 22 to 48 hours. P-T-H_2O parameters were chosen so that the experiments were conducted at volatile-undersaturated conditions. All runs were terminated by drop quench and the capsules were reweighed at the end of the experiments. All capsules showed no weight loss upon piercing (followed by 5 minutes in an oven at 120°C), confirming that they were volatile undersaturated and therefore all the H_2O-NaBr fluid was incorporated in the melt at the target P-T conditions. Synthesized glasses are crystal- and bubble-free, except for the rhyodacitic glasses, which include some spherical air bubbles.

3. Geochemical characterization of the glasses: analytical methods

3.1 Electron Microprobe (EMP)

The major element composition of each glass (Table 2) was analysed with a SX Five Cameca electron microprobe at ISTO (Orléans, France), using the following operating conditions: 15 kV accelerating voltage, 4-6 nA beam current, 10 s counting time on peak and 5 s on background for all elements on each spot, and 12-20 µm spot size. Sodium was analysed first to limit any loss.

Br analysis was also attempted in the Br-richest basaltic glass (B6000: 5968 ppm Br; Table 2 and 3). The Lα1 (1.480 keV) and the Lβ1 (1.526 keV) Br X-ray emission lines were investigated using a LTAP crystal (peak position: sin θ = 0.32481 and 0.32480, respectively) and a focused beam, at 10, 12 or 15 kV accelerating voltage and 10 or 20 nA beam current.

The dwell time was set to 100 seconds for 1,000 points. Under all conditions, the Lα1 line of Br was invisible in the basaltic glass (Fig. S1 in Supplementary material), because it was hidden by the Kα line of Al (1.487 keV). Due to the extremely high abundance of Al in the glass, the quantification of Br is impossible even by correcting for the interference.

The Kα line of Br (11.907 keV) was also explored in the B6000 glass using a LLIF crystal (peak position: sin θ = 0.25825) and a focused beam, at 25 kV and 20 nA: the peak is visible, without interferences, but has a very low intensity (< 200 counts per second). The quantification of Br contents of at least several thousand ppm is therefore possible by using long counting times. This has been previously suggested by Bureau et al. (2000), who analysed 2580 ppm Br in a Na_2O-SiO_2-Al_2O_3 glass at 20 kV, 50 nA, 40 μm spot size and 100-200 s counting time. However, Br contents < 1000 ppm are likely impossible to be measured using this technique (Bureau et al., 2000), and therefore we did not conduct a proper quantification of Br in our set of standards using EMP.

3.2 Secondary Ion Mass Spectrometry (SIMS)

The analysis of water dissolved in the glasses was performed with a Cameca IMS 1280 HR2 at Centre de Recherches Pétrographiques et Géochimiques (Nancy, France). Spot analyses of secondary ions ^{17}O, $^{16}O^{1}H$, ^{18}O, ^{29}Si, ^{30}Si were obtained using a 3 nA, 20 μm diameter primary beam of Cs^+ ions. The electron gun was simultaneously used for charge compensation. The measurements were made at a mass resolution of ~7700, to separate $^{17}O^-$ and $^{16}O^{1}H^-$. Energy filtering was set at +30 ±10 eV by moving the energy slit off axis, to minimize both matrix effect and instrumental background. A 10 × 10 μm raster was used for 1 minute prior to analysis at each spot in order to pre-sputter through the gold coat and remove surface contamination. The beam position in the field aperture and the magnetic field centering was checked before each measurement. Each analysis on one spot consisted of 18 cycles of measurements, with counting times and switching times of 3 and 1 s respectively at each peak.

Concentrations of H_2O (Table 2) were calculated using a best-fit quadratic polynomial regression to count-rate ratios (normalized to ^{30}Si) versus variable known concentration ratios (referenced to wt% SiO_2) of experimental glass standards of basaltic (sample N72, Kamtchatka; Shishkina et al., 2010), trachy-andesitic (sample TAN25, Tanna Island, Vanuatu; Metrich & Deloule, 2014), dacitic and rhyolitic (Pinatubo, Philippines; Scaillet & Evans, 1999) compositions, with H_2O contents ranging from 0 to ~6 wt%.

3.3 Instrumental Neutron Activation Analysis (INAA)

Br content of all standards was quantified using INAA. Analyses of basaltic glasses were performed by Actlabs (Ancaster, Canada). The method is described by Hoffman (1992). About 300 mg of glass was weighed into small polyethylene vials specifically fabricated for Actlabs for low background. Samples were irradiated with control international reference material CANMET STSD-2 and NiCr flux wires at a thermal neutron flux of 7×10^{12} $n.cm^{-2}.s^{-1}$ in the McMaster Nuclear Reactor. Following a 7-day-decay, the samples were measured on an Ortec high purity Ge detector with a resolution of 1.67 keV for the 1332 keV Co-60 photopeak. The detector is linked to Canberra Series 95 multi-channel and is fully computer automated. Activities for each element are decay- and weight-corrected and compared to a detector calibration developed from multiple international certified reference materials. STSD-2 (stream sediment reference material) is used as a control to verify the system is operating properly. Selected samples were re-measured and compared to the original as part of the Quality Assurance procedure.

INA analyses for andesitic and rhyodacitic glasses were done at the University of Massachusetts Lowell Radiation Laboratory (USA). Approximately 200 mg of glass powder was weighed into 1.5 mL acid leached high-purity polyethylene vial. Iron wires were attached to each vial to serve as neutron dose monitors. The samples were irradiated in the UMass Lowell 1 Mw research reactor for 2 hours at a flux of 1×10^{13} $n \cdot cm^{-2} \cdot s^{-1}$. After irradiation the samples were transferred to un-irradiated polyethylene vials. This was done because earlier work had shown that Br does occur in polyethylene. However, subsequent analysis of the high purity polyethylene vials obtained from ActLabs revealed that Br content in the vials was 0.03 ppm. Thus sample transfer is an unnecessary step except for samples that have Br concentrations near the detection limit.

Samples were counted 5 to 6 days after irradiation for 10,000 seconds on a Broad Energy Germanium Detector (Canberra Instruments). Gamma ray energies and peak areas were determined using Genie 2000 software (Canberra Instruments). For Br determinations, the isotope of interest is ^{82}Br. There are a number of potential analytical gamma ray peaks for this isotope. In our work we used the 554.35 keV and 776.52 keV gamma ray peaks which are the most intense peaks in the gamma ray spectrum. If the sample contains W, the third most intense peak, 619.11 keV, should not be used because of the significant interference due to the 618.26 keV ^{186}W gamma ray. Note that with a half-life of 23.72 hours (^{82}Br has half-life of 35.28 hours), and a significant thermal neutron capture cross-section for this isotope, the ^{186}W

gamma ray interference will persist throughout the optimum counting window (4-7 days) for ^{82}Br. The other gamma rays in the ^{82}Br spectrum yield reasonable results but, because of their lower relative intensities, there is a greater analytical uncertainty associated with these gamma ray energies.

Decay, flux and geometry corrections were done using in-house software. Bromine concentrations were determined by reference to the USGS geochemical standard MAG-1. The reported Br content for this sample ranges from 232 to 251 ppm (GeoRem database). We have determined the Br content for this reference standard using a primary standard (DIONEX Combined 7-anion Standard II) which is directly referenced to NIST SRM 3184. Our new value for MAG-1 is 222 ± 3 ppm. This value was used to calculate the Br concentrations in the glasses.

4. Bromine measurement by *in-situ* analytical methods

4.1 Synchrotron X-Ray Fluorescence (SR-XRF)

Bromine in the basaltic standards was analysed via SR-XRF at the UK national synchrotron facility, Diamond Light Source (Didcot, Oxfordshire). The Diamond Light Source has been operating with a circulating 3 GeV electron beam in its storage ring since September 2006. The analyses were performed on I18, the Microfocus Spectroscopy beamline (Mosselmans et al., 2009), which provides a high-brightness micron-sized X-ray beam for quantitative, non-destructive elemental analysis with high sensitivity (sub-ppm detection limit) and high spatial resolution (e.g., Berlo et al., 2013). The source of the high brightness photon beam is an undulator and the focusing of the X-ray beam on the sample is achieved by a pair of Kirkpatrick Baez (KB) mirrors.

The analyses were performed on small glass chips (30-100 μm in thickness) embedded in Epofix Resin supports. For the measurements described here a beam of approximately 5×5 μm^2 was used and the analysis time was 120 seconds. The measurements were performed in fluorescence mode (sample at 45 degrees to both the beam and the detector). A nine-element Ortec germanium detector was used. The energy of the beam on the sample was tuned at 15

keV. An aluminium filter in front of the detector ensured reduction of the substantial Fe signal to prevent saturation of the detector and promote Br signal-to-noise ratio.

The acquired fluorescence spectra were processed by PyMca (Sole et al., 2007), an open source X-ray Fluorescence Toolkit developed by the Software Group of the European Synchrotron Radiation Facility (ESRF). In the raw spectra, the K-lines of Br in the sample were identified and an iterative peak fitting procedure applied to reveal the net peak areas free of background and interference from other elements. The Br net peak area of the sample was obtained after the subtraction of the net peak area of the blank (Table S1), which accounted for the signal from the resin underlying each standard. Each basaltic standard was measured in 4 individual spots to check analytical reproducibility. Quantification of Br was then achieved by comparing the combined peak area at 11.88 and 11.92 keV (the K-alpha lines of Br) to the Br loaded into the capsules.

4.2 Laser ablation inductively coupled plasma mass spectrometry (LA-ICP-MS)

We analyzed the bromine contents of the Br-doped glasses by LA-ICP-MS at the Istituto Nazionale di Geofisica e Vulcanologia (INGV, Palermo, Italy). Small glass pieces of the three sets of standards were mounted and polished in Epofix Resin. We employed a Compex Pro 102, 193 nm ArF excimer laser mounted on an ablation system GeoLas Pro provided by Cetac, which includes a small volume (< 5 cc) aluminium ablation cell covered by a quartz glass lid transparent to UV light (enabling high signal/noise ratios and preventing organic material contamination of the samples). The cell is connected to an Agilent 7500ce Inductively Coupled Plasma Mass Spectrometer with a Teflon tube having a 3 mm internal diameter. This set-up is routinely used for major and trace elements measurement in crystals and glasses. The biggest challenge in Br detection by LA-ICP-MS derives from the high ionization potential of this element (11.81 eV), close to that of the Ar (15.76 eV) plasma source and resulting in relatively low sensitivities. Using a standard configuration (see Correale et al., 2012), both ^{79}Br and ^{81}Br isotopes presented very high background signals, preventing analyses at concentrations lower than 1000 ppm Br. Several configuration parameters were therefore tested, following the procedure described by Seo et al. (2011), in order to achieve the best setting to avoid interferences with other masses, to obtain the highest

signal/blank ratio (i.e. the ratio of the intensity measured on a Br-doped sample to the intensity measured on a sample without Br), and to reduce the sputtering of material around the ablation hole. The preferred configuration was: fluency energy: 15 J/cm^2, pulse energy: 100 mJ, pulse duration: 15 ns, pulse repetition rate: 10 Hz, spot diameter: 90 µm (the smallest spot allowing a good signal in Br-poor glasses), ablation duration: ~50 s, gas carrier flux: 800 ml He/min, RF power: 1500 W, plasma gas: 15 l Ar/min, make up gas: 0.5 l Ar/min, dwell time: 10-80 ms.

The resolution and the mass axis were tuned with a 50 ppm Br solution in order to enhance the signal of the two isotopes, ^{79}Br and ^{81}Br, affected by interferences with ^{40}Ar^{40}Ar, ^{39}Ar^{40}Ar, and ^{40}Ar^{40}ArH, which increases the background of these two masses. Then we optimized the ICP-MS parameters (e.g., ion lens voltage, Electron Multiplier voltage, torch position, gas flow rates) by ablating a NIST SRM 610 glass. The carrier gas flow in the torch was adjusted to have ThO/Th ratios < 1 %. Signal detection was performed in ion counting mode.

We meticulously cleaned the sample cell before and after each analytical session by using a dilute nitric acid solution followed by ethanol or acetone. Each analysis lasted about 2 minutes: one minute of background signal acquisition, followed by ~50 seconds of ablation. Data were collected in time-resolved graphics in order to evaluate signal stability, to detect possible inhomogeneities during the ablation, and to select the most reliable portions of the signal over time. Quantification of Br was achieved by comparing the ratio of Br and Mg signals (in counts per second) measured by the LA-ICP-MS to the nominal content (in ppm) of Br (i.e., the amount loaded in the capsule). We also performed data reduction using GLITTER™, a software for the laser ablation microprobe, developed by the ARC National Key Centre for Geochemical Evolution and Metallogeny of Continents and Exploration and Mining (Griffin et al., 2008). For all the glasses we analysed, we used ^{24}Mg (from the EMP analyses; Table 2) as the reference element, after having verified that the choice of the reference element does not significantly modify the results.

4.3 Secondary Ion Mass Spectrometry (SIMS)

Br analyses were also performed by SIMS with a Cameca IMS 1280 HR2 at the French national SIMS facility (Centre de Recherches Pétrographiques et Géochimiques, Nancy).

Polished chips of basaltic, andesitic and rhyodacitic standard glasses were set into indium and coated with gold. The Cs+ primary ion beam was accelerated at 10 kV with an intensity of 5 nA and focused on a 15 µm diameter area. The electron gun was simultaneously used for charge compensation. Negative secondary ions were extracted with a 10 kV potential, and the spectrometer slits set for a mass resolving power (MRP = M/ΔM) of ~20,000 to separate isobaric interferences of hydrides (Se H), oxides (Cu O), and metal (Fe Mg, V Mg, Cr Al and Fe Al) from Br. The field aperture was set to 2500 µm, and the transfer optic magnification adjusted to 200. Rectangular lenses were activated in the secondary ion optics to increase the transmission at high mass resolution (de Chambost et al., 1996). $^{28}Si^{16}O_3^-$ (75.963 amu) was measured as an internal reference to determine the Br contents (SiO_2 of the glasses is known by EMPA, Table 2), $^{30}Si^{16}O_3^-$ (77.959 amu) to verify the $^{30}SiO_3^-/^{28}SiO_3^-$ isotopic ratio, and $^{79}Br^-$ and $^{81}Br^-$ to calculate $^{81}Br/^{79}Br$ ratio (as an indicator of potential isobaric interferences or analytical artefacts). The measurements were realized by peak jumping in monocollection mode by ion-counting. Each analysis consisted of 6 to 8 successive cycles. Each cycle began with a background measurement at mass 75.8, followed by $^{28}Si^{16}O_3^-$, $^{30}Si^{16}O_3^-$, $^{79}Br^-$ and $^{81}Br^-$, with measurement times of 4, 4, 4, 10 and 30 s, respectively (waiting time of 2 s). The beam position in the aperture field and contrast aperture, and the mass calibration were checked before each measurement, after a 30 s pre-sputtering with a 10 µm rastering. The energy window was opened at 20 eV, and its low energy side was positioned at a 30 eV offset, to minimize the matrix effect.

The count rate measured for a Br isotope depends on the Br concentration in the target material, the amount of material sputtered, and the ionization yield of the element. In measuring together with Br a compound of known concentration (SiO_3 in our case), the concentration of Br in the sample can be calculated following Shimizu et al. (1978).

Two MPI-DING (Max-Planck-Institut für Chemie – Dingwell) reference glasses with Br contents ≤ 1.2 ppm (Jochum et al., 2006) were also analyzed during a separate session with the same analytical conditions: ATHO-G (1.2 ppm Br, 75.6 wt% SiO_2) and StHs6/80-G (0.8 ppm Br, 63.7 wt% SiO_2).

5. Results

5.1. Homogeneity of the synthesized glasses

The homogeneity of the Br content of the glasses was evaluated by SIMS. Profiles with 5-20 points were performed across the glass chips (~1-5 millimeters in size) of 16 glasses (Table S2). With a spot size of 15 μm, potential inhomogeneities at the μm scale are not detectable.

The internal analytical error on the measurement of the $^{79}Br/SiO_3$ ratios is generally 2-3 % (Table S2). For most of the glasses, the Relative Standard Deviation (RSD) on the average $^{79}Br/SiO_3$ ratio is less than 6 %, and the external error (2σn) less than 5 %; only sample B10 has a RSD of 10% and a 2σn of 7 % (Table S2). For 6 of the 16 analyzed glasses, the external error is therefore equal to or lower than the internal error (Table S2), and for the other glasses slightly higher. We therefore consider that all the glasses are reasonably homogeneous, and the variation in their Br content is less than 10%.

We also checked for possible gradients in the Br contents due to the occurrence of bubbles in the rhyodacitic glasses. The profile that we did between two bubbles of sample RD500 does not show any variation (RSD = 0.9 %, Table S2).

5.2. Bromine characterization

Table 3 and Figure 1 show the good agreement for andesitic and rhyodacitic samples between the amount of Br loaded in every capsule and the Br content measured in the glass by INAA (accuracy ≤ 12% and relative precision ≥ 2%). The agreement is still acceptable (accuracies between 4 and 32%) for basaltic samples with Br contents ≥ 100 ppm, while INAA results clearly overestimate loaded amounts of Br in basaltic samples with less than 100 ppm Br. A possible explanation of this overestimation is a high background signal due to the high Light Rare Earth Elements (LREE) content (i.e., high activity) of the basalt (twice the LREE contents of the andesite, Table 1).

In samples with high total rare earth element, and particularly a high Light REE content, Br sensitivity of the INAA method is limited by the overall activity of the sample. Both ^{139}La and ^{152}Sm have large capture cross-sections for neutrons and radioactive half-lives that are greater than that of ^{82}Br. Modern gamma ray detectors and the associated electronics can handle relatively high dead times, but our experience has led us to conclude that dead times of greater than 15% should be avoided. This means that for high LREE samples (total LREE greater than several hundred ppm) there needs to be a significant increase in the detector-sample

spacing which correspondingly decreases the total counts for the various ^{82}Br gamma rays (the inverse square law in action). Depending on the activity of the specific sample, detection limits for Br can increase by several orders of magnitude from 0.1 ppm (for low activity sample) to the 10 to 20 ppm range. Thus for samples with high LREE content (>> 100 ppm) and low Br content (< 10 ppm) INAA is not an analytical method of choice as was demonstrated for apatites (Marks et al., 2012), and as demonstrated here with the basaltic glasses with Br ≤ 50 ppm.

5.3. Results obtained with the micro-analytical techniques

In order to have a coherent dataset of Br values for all the standards, we use loaded Br values to compare SR-XRF, LA-ICP-MS and SIMS results. Loaded Br contents are initially compared to the signals measured with the three different techniques (Figs. 2, 3, 4). The net peak area after blank subtraction from SR-XRF analyses and ^{79}Br (cps) /^{24}Mg (cps) from LA-ICP-MS analyses are plotted versus nominal values (Figs. 2 and 3, respectively), while the relative sensitivity factor for Br relative to SiO_3 (^{79}Br/SiO_3) from SIMS analyses are plotted against known Br (nominal, ppm)/SiO_2 (measured, wt%) ratios (Fig. 4). Ratios to a reference element are necessary in the case of LA-ICP-MS and of SIMS to normalize measurements with respect to the ablated volume (Gunther et al., 1998). Figures 2, 3 and 4 show that the relationships are linear in all cases and, when different compositions are analysed (basalt, andesite and rhyodacite), they show different slopes (Figs. 3 and 4a). For LA-ICP-MS and SIMS data the same calibration curve (passing through the origin) accounts for standards with high and low Br concentrations (Figs. 3b and 4b). For SR-XRF data a different linear calibration is needed for the very low Br concentrations (≤ 12 ppm; Fig.2b). The regression curves of the experimental data are used to recalculate Br contents, listed in Table 3, from the mean of *n* analyses on a given standard.

Figure 5 (a, b) shows calculated Br contents versus nominal concentrations (Br loaded into the capsule), for the three different methods. A good agreement between the three datasets is shown by glasses with Br contents > 500 ppm (Fig. 5a). The glasses with lower contents have a greater scatter (Fig.5b). The accuracy of the three methods is estimated by computing the relative difference between the calculated Br content and the nominal value (Fig. 5c): the accuracy is generally better for SR-XRF data for a given Br content. Hereafter we discuss the results obtained by each technique more in detail.

LA-ICP-MS

Raw Br/Mg ratio shows a linear relationship with the nominal Br content from ~100 up to ~6000 ppm (Fig. 3a). We did not analyze any sample containing less than 100 ppm Br, therefore we cannot estimate the Br detection limit with this technique. The contents of standard glasses with Br > 100 ppm were reproduced with accuracies ≤ 14 % and precisions better than 19 %.

It should be noted that LA-ICP-MS raw data were also processed using the GLITTER™ software, using one of the basaltic glasses as a single external standard (Table S3). Predictably, the closer the Br content of the external standard was to that of the sample, the more accurate the value estimated by GLITTER™. Two external standards were tested, B3000 and B1000 (nominal Br contents of 2690 ppm and 967 ppm, respectively): when B3000 is used, the content of the highest concentration glass (5968 ppm) is well reproduced, but not those of glasses with lower concentrations (≤ 967 ppm); when B1000 is used, the concentration of the glasses with the nearest contents (593 ppm and 2690 ppm) are well reproduced, but not those of the glasses with the more different concentrations (5968 ppm and ≤ 294 ppm; Table S3). The matrix effect has been estimated to be negligible in the estimations performed with GLITTER™: employing the B1000 basaltic glass as an external standard, the quantification of similar Br contents in glasses of andesitic and rhyodacitic compositions (RD100, RD500, RD5000, A500, A1000) was as accurate as those in the basaltic glasses (Table S3).

SIMS

Reported in a log-log plot (Fig. 4a), the measurements of the standard glasses define a linear relationship over several orders of magnitude, pointing to the absence of instrumental saturation or instrumental background. On a normal linear plot (Fig. 4b), the basaltic glasses and the rhyodacitic glasses define distinct regression lines, with a decrease of the relative Br ionization yield of 33% from basaltic to rhyodacitic composition, due to both a decrease of the Br ionization yield and an increase of the SiO_3 ionization yield.

The Br contents determined by SIMS approach the nominal contents for the standards with Br > 100 ppm (accuracy < 25 %; Table 3) and are generally consistent with the contents determined by LA-ICP-MS (Fig. 5a, b). Br measurements in samples with Br contents ≤ 100 ppm are less accurate. Br contents ≥ 10 ppm are measured with a precision < 10%, and Br contents < 10 ppm with a precision of ≤ 20%.

The Br detection limit of SIMS technique was tested by analyzing two MPI-DING reference glasses with Br contents ≤ 1.2 ppm (ATHO-G and StHs6/80-G; Jochum et al., 2006). The counting rate on ^{79}Br and ^{81}Br are close to 200 cps, the measured $^{79}Br/^{81}Br$ ratio close to the true value (± 10 %, thus indicating the absence of isobaric interferences or analytical artifacts) and the relative error on the Br/SiO_3 ratio is about 2 % (Table 4). Br contents were calculated using the new set of andesitic and rhyodacitic standards presented in this study. The Br contents of the two MPI-DING glasses were reproduced with accuracies of 16-19% and precisions of 2-5% (Table 4). Therefore, it seems possible to measure Br contents of the order of 1 ppm with a reasonable accuracy (≤ 20 %). With counting rates of about 40 cps/nA/ppm as observed in this study, it may be expected that Br contents as low as 100 ppb can be determined by SIMS, with spot size in the range of 20 µm.

Note that Marks et al. (2012) achieved a similar detection limit (≤ 1 ppm) for Br measurement on apatite by SIMS, by using a low mass resolution and peak stripping to remove CaCl isobaric interferences, an analytical protocol not adapted to glasses with more complex and variable chemical compositions, and more interfering species.

SR-XRF

Blank-subtracted peak areas for the basaltic standards analysed by SR-XRF are linearly correlated with Br nominal concentrations (Fig. 2a). A good correlation ($R^2 = 0.97$) was also obtained at the sub-12 ppm level (Fig. 2b). Br contents for the standards with more than 12 ppm Br (B50 to B6000) and less than 12 ppm Br (B0.5 to B10) standards were calculated using the equations of the regression lines in Figures 2a and 2b.

We estimate that the experimental setup used with SR-XRF allowed detection limits lower than 1 ppm, although the low concentration glasses used are not fully characterized (section 5.2). This estimate is based on the Br-poorest standard (B0.5: 0.5 ppm Br). The epoxy resin

used to embed the samples contained traces of Br, however the B0.5 signal was still above that of the blank. The signal from the resin underlying each standard is likely attenuated by the basalt (attenuation length for Br in basalt is around 150 μm) therefore its contribution to the total Br peak of the glasses is likely further reduced. The potential contribution of the resin was however still accounted for by subtracting the Br net peak area of the blank from that of the standards (as shown in Table S1).

The contents of standard glasses with loaded Br ≤ 10 ppm are determined by SR-XRF with a better accuracy than with SIMS (Fig. 5c), but the precisions of the two methods are similar (Table 3). Br contents > 10 ppm are measured by SR-XRF with a precision < 10% (similar to the SIMS), and Br contents < 10 ppm with a precision < 30%.

6. Discussion

6.1. Produced standards

EMP and SIMS analyses showed that our Br-doped glasses have homogeneous compositions in terms of major element and Br contents (Tables 2 and 3). INAA confirmed, with accuracy better than 32%, nominal Br contents (i.e. the amount of Br loaded in the experimental charge) of 16 glasses out of 21 (the Br contents of 15 glasses are confirmed with accuracy better than 20 %). We have therefore produced a new set of 16 standard glasses for Br, with variable compositions and Br contents: 5 rhyodacitic glasses with Br contents varying from 10 to 5640 ppm Br, 5 andesitic glasses with Br contents between 11 and 1110 ppm Br, and 6 basaltic glasses with Br contents between 118 and 6930 ppm Br. The nominal Br contents of 5 basaltic glasses with Br between 0.5 and 52 ppm were not corroborated by INAA (Table 3). We will nevertheless discuss the results obtained analysing these glasses by SR-XRF and SIMS, because (i) the uncertainty in the loaded Br content in these samples is lower than 5.5% (Table 3), as for the high concentration samples (it does not depend on Br value), and (ii) SR-XRF and SIMS data do not show any clear evidence of "anomalous" contents (Table 3).

6.2. Applicability

These standard glasses can be used to quantify Br abundances of experimental and natural glasses using *in-situ* analyses. The tests we performed with LA-ICP-MS on some of our standards show that this method is well suited to analyse Br-doped (> 100 ppm) super liquidus or sparsely phyric experimental charges. With a 90 µm spot size, Br contents of hundreds to thousands of ppm are quantifiable with accuracy within 14 % (Fig. 5c). Smaller spot sizes significantly reduced the quality of the analyses. The use of a single external standard allows an accurate quantification if the Br content of the standard is similar to the Br contents of the samples (Table S3). The composition of the external standard does not seems to be crucial since the Br contents of the andesitic and rhyodacitic glasses have been properly quantified using a basalt standard in GLITTER™ calculations (Table S3). However, if Br contents vary by more than 40% among the samples, it is preferable to use a set of standards with various Br contents in order to build a calibration line (as in Fig. 3).

The LA-ICP-MS method needs further developments to improve its range of application, notably to measure Br contents in natural silicate glasses. With an ablation diameter of 90 µm, the method is currently unsuited to analyse Br contents in melt inclusions and interstitial glasses of volcanic samples, which are most often a few tens of microns in size and generally contains a few to a few tens ppm of Br (Bureau and Metrich, 2003; Kutterolf et al., 2013, 2015). Previous studies on scapolite, amphibole and sodalite minerals and on fluid inclusions determined very low detection limits: 4-15 ppm (Seo et al., 2011; Hammerli et al, 2013). In comparison to these two studies, we observed (i) a slightly higher background, i.e. the Br signal while gas carrier fluxes the sample cell without any ablation (which is typical of each ICP-MS), but also (ii) a higher blank, i.e. the Br signal during ablation of a Br-free sample (probably owing to a lower production of interfering masses with fluid inclusions or minerals than with silicate glasses).

In recent works, the SR-XRF has been preferentially used to analyse the low Br contents in melt inclusions and glassy matrices of volcanic rocks (e.g., Costa, 2014; Kutterolf et al., 2013, 2015). Among the methods used in this study, the SR-XRF is the best suited for analysing natural samples. It has the advantage of a high spatial resolution (in this study, 5×5 µm), a very low Br detection limit (< 1 ppm), and it is non-destructive. Analyses performed with this method present the best accuracy (<10% for Br ≥ 10 ppm; >20% for Br ≤ 5 ppm) and a good

precision (< 10% for Br > 10 ppm, > 30% for Br < 10 ppm). The SR-XRF method is of course appropriate also to characterize experimental samples, its main drawbacks being the accessibility and the cost.

SIMS requires several standards with chemical compositions close to the samples. The secondary ion intensity is linearly correlated to the Br content over the entire concentration range for each composition. This means that few standards are required to draw a calibration line and extrapolations to low or higher concentrations are possible. Indeed, here we demonstrate that using our andesitic and rhyodacitic set of standards, the lowest Br contents of which is 10 ppm, it is possible to determine Br contents as low as 1 ppm with an accuracy < 20% and a precision < 5%. With a spatial resolution of ~15 μm and a Br detection limit ≤ 1 ppm, SIMS is an appropriate technique to analyze natural volcanic glasses. Additionally, it has the advantage of simple data processing and it is more readily available than SR-XRF.

7. Conclusions

We produced a set of homogeneous standard glasses with basaltic, andesitic and rhyodacitic compositions and Br contents varying from 0.5 to 6,000 ppm. The nominal Br contents (amounts of Br loaded in the experimental samples) of 15 out of 21 standards were confirmed by INAA. These standards can be used to quantify the Br contents in silicate glasses by *in-situ* techniques. Our measurements show that (i) the SR-XRF method is currently the most suited to analyse low Br contents in melt inclusions and matrix glasses of volcanic rocks; (ii) at its present stage of development, LA-ICP-MS is an accessible method that can be used to measure hundreds to thousands ppm Br in experimental glasses; (iii) SIMS is a very promising method to analyse low bromine contents in natural volcanic glasses and other geological materials, once its accuracy is improved, and it presents the advantage of being more accessible than SR-XRF.

Small amounts of the standard glasses can be obtained on request to the corresponding author.

Acknowledgements

This work was partly funded by the "Laboratoire d'Excellence VOLTAIRE" (Université d'Orléans, France) and by the ANR-12-JS06-0009-01 project InterVol. A.C. thanks J.L. Devidal (LMV, Clermont-Ferrand) for interesting exchanges about LA-ICP-MS Br measurements and for performing some trace element measurements in andesitic and rhyodacitic standard glasses. J. Andujar (ISTO, Orléans) provided the andesitic (USC-2) starting dry glass. A.P. is grateful to M. Walle (ETH, Zurich) for useful suggestions. A.A., K.B, K.G., T.A.M. and D.M.P. acknowledge the Diamond Light Source for time on Beamline I18 under Proposal sp8797. A.A. and K.B. acknowledge the European Research Council under the European Union's Seventh Framework Programme (FP7/2007/2013)/ERC grant agreement n° 305377 (PI, Aiuppa) and 307356 (PI, Berlo) and G.N.E. acknowledges the support of the Radiation Laboratory at the University of Massachusetts Lowell. P. Sarda (Université Paris Sud XI, Orsay) is thanked for his proofreading of the manuscript.

References

Aiuppa, A., Baker, D.R. and Webster, J.D., 2009. Halogens in volcanic systems. Chem. Geol., 263(1-4): 1-18.

Baker, D.R. and Alletti, M., 2012. Fluid saturation and volatile partitioning between melts and hydrous fluids in crustal magmatic systems: The contribution of experimental measurements and solubility models. Earth-Sci. Rev., 114(3-4): 298-324.

Balcone-Boissard, H., Michel, A. and Villemant, B., 2009. Simultaneous Determination of Fluorine, Chlorine, Bromine and Iodine in Six Geochemical Reference Materials Using Pyrohydrolysis, Ion Chromatography and Inductively Coupled Plasma-Mass Spectrometry. Geostandards and Geoanalytical Research, 33(4): 477-485.

Berlo, K. et al., 2013. Element variations in rhyolitic magma resulting from gas transport. Geochim. et Cosmochim. Acta, 121: 436–451.

Bobrowski, N., Hönninger, G., Galle, B. and Platt, U., 2003. Detection of bromine monoxide in a volcanic plume. Nature, 423: 273–276.

Boulyga, S.F. and Heumann, K.G., 2005. Direct determination of halogens in powdered geological and environmental samples using isotope dilution laser ablation ICP-MS. Int. J. of Mass Spectrom., 242(2-3): 291-296.

Bureau, H., Keppler, H. and Métrich, N., 2000. Volcanic degassing of bromine and iodine: experimental fluid/melt partitioning data and applications to stratospheric chemistry. Earth and Planet. Sci. Letters, 183(1-2): 51-60.

Bureau, H. and Métrich, N., 2003. An experimental study of bromine behaviour in water-saturated silicic melts. Geochim. et Cosmochim. Acta, 67(9): 1689-1697.

Bureau, H. et al., 2010. Bromine cycle in subduction zones through in situ Br monitoring in diamond anvil cells. Geochim. et Cosmochim. Acta, 74(13): 3839-3850.

Cadoux, A., Scaillet, B., Druitt, T.H. and Deloule, E., 2014. Magma storage conditions of large Plinian eruptions of Santorini Volcano (Greece). J. of Petrol., 55(6): 1129-1171.

Cadoux, A., Scaillet, B., Bekki, S., Oppenheimer, C. and Druitt, T.H., 2015. Stratospheric Ozone destruction by the Bronze-Age Minoan eruption (Santorini Volcano, Greece). Sci. Rep., 5: 12243. In press, doi: 10.1038/srep12243.

Correale, A. et al., 2012. New evidence of mantle heterogeneity beneath the Hyblean Plateau (southeast Sicily, Italy) as inferred from noble gases and geochemistry of ultramafic xenoliths. Lithos, 132-133: 70-81.

Costa, M., 2014. Bromine degassing in basaltic volcanic systems. Dottorato di Ricerca in Geochimica - XXIV ciclo Thesis, University of Palermo, Palermo, 126 pp.

Daniel, J.S., Solomon, S., Portmann, R.W. and Garcia, R.R., 1999. Stratospheric ozone destruction: The importance of bromine relative to chlorine. J. Geophys. Res., 104: 23871–23880.

de Chambost, E., Schumacher, M., Lovestam, G. and Claesson, S., 1996. Achieving high transmission with the Cameca IMS 1270, in: Benninghoven, A., Hagenhoff, B., Werner, H.W. (Eds.), Secondary Ion Mass Spectrometry, SIMS X. Wiley, Chichester, pp. 1003-1006.

Gerlach, T.M., 2004. Volcanic sources of tropospheric ozone-depleting trace gases. Geochem., Geophys., Geosystems, 5: Q09007.

Gunther, G., Audetat, A., Frischknecht R., and Heinrich C., A. 1998. Quantitative analysis of major, minor and trace elements using laser ablation inductively coupled plasma mass spectrometry, Journal of Analytical Atomic Spectrometry, 13: 263-270.

Griffin, W.L., Powell, W.J., Pearson, N.J., O'Reilly, S.Y., 2008. Glitter: data reduction software for laser ablation ICP-MS. In/ Sylvester, P. (Ed.), Laser Ablation ICP-MS in the Earth Sciences: Current Practices and Outstanding Issues: Mineralogical Association of Canada, Short Course Series, 40: 308-311.

Hammerli, J., Rusk, B., Spandler C., Emsbo P., Oliver, N.H.S., 2013. In situ quantification of Br and Cl in minerals and fluid inclusion by LA-ICP-MS: A powerful tool to identify fluid sources. Chem. Geol., 337-338: 75-87.

Hoffman, E.L., 1992. Instrumental Neutron Activation in Geoanalysis. J. of Geochem. Explor., 44: 297-319.

Iacono-Marziano, G., Morizet, Y., Le Trong, E. and Gaillard, F., 2012. New experimental data and semi-empirical parameterization of H_2O-CO_2 solubility in mafic melts. Geochim. et Cosmochim. Acta, 97: 1-23.

Jambon, A., Déruelle, B., Dreibus, G. and Pineau, F., 1995. Chlorine and bromine abundance in MORB: the contrasting behaviour of the Mid-Atlantic Ridge and East Pacific Rise and implications for chlorine geodynamic cycle. Chem. Geol., 126(2): 101-117.

Jochum, K.P. et al., 2006. MPI-DING reference glasses for in situ microanalysis: New reference values for element concentrations and isotope ratios. Geochemistry, Geophysics, Geosystems, 7(2): Q02008.

Kendrick, M.A., 2012. High precision Cl, Br and I determinations in mineral standards using the noble gas method. Chemical Geology, 292-293: 116-126.

Kutterolf, S. et al., 2013. Combined bromine and chlorine release from large explosive volcanic eruptions: A threat to stratospheric ozone? Geology, 41(6): 707–710.

Kutterolf, S. et al., 2015. Bromine and chlorine emissions from Plinian eruptions along the Central American Volcanic Arc: From source to atmosphere. Earth and Planetary Science Letters, 429: 234-246.

Lesne, P., Scaillet, B., Pichavant, M., Iacono-Marziano, G. and Beny, J.-M., 2011a. The H_2O solubility of alkali basaltic melts: an experimental study. Contrib. to Mineral. and Petrol., 162(1): 133-151.

Lesne, P., Scaillet, B., Pichavant, M. and Beny, J.-M., 2011b. The carbon dioxide solubility in alkali basalts: an experimental study. Contrib. to Mineral. and Petrol., 162(1): 153-168.

Longerich, H.P., Jackson, S.E., Fryer, B.J. and Strong, D.F., 1993. The laser ablation microprobe inductively coupled plasma-mass spectrometer. Geosci. Can., 20: 21-27.

Marks, M.A.W. et al., 2012. The volatile inventory (F, Cl, Br, S, C) of magmatic apatite: An integrated analytical approach. Chem. Geol., 291: 241-255.

Marks, M.A.W., Kendrick, M.A., Eby, G.N., Zack, T. and Wenzel, T., 2016. The F, Cl, Br and I Contents of Reference Glasses BHVO-2G, BIR-1G, BCR-2G, GSD-1G, GSE-1G, NIST SRM 610 and NIST SRM 612. Geostandards and Geoanalytical Research: doi: 10.1111/ggr.12128.

Métrich, N. and Deloule, E., 2014. Water content, δD and δ11B tracking in the Vanuatu arc magmas (Aoba Island): Insights from olivine-hosted melt inclusions. Lithos, 206-207: 400-408.

Millard, G.A., Mather, T.A., Pyle, D.M., Rose, W.I. and Thornton, B., 2006. Halogen emissions from a small volcanic eruption: Modeling the peak concentrations, dispersion, and volcanically induced ozone loss in the stratosphere. Geophys. Res. Lett., 33(19): L19815.

Mosselmans, J.F.W. et al., 2009. I18 – the microfocus spectroscopy beamline at the Diamond Light Source. J. of Synchrotron Radiat., 16: 818-824.

Oppenheimer, C. et al., 2006. BrO formation in volcanic plumes. Geochim. et Cosmochim. Acta, 70(12): 2935-2941.

Oppenheimer, C. et al., 2010. Atmospheric chemistry of an Antarctic volcanic plume. J. of Geophys. Res., 115: D04303.

Pyle, D.M. and Mather, T.A., 2009. Halogens in igneous processes and their fluxes to the atmosphere and oceans from volcanic activity: A review. Chem. Geol., 263(1-4): 110-121.

Ruzié-Hamilton, L. et al., 2016. Determination of halogen abundances in terrestrial and extraterrestrial samples by the analysis of noble gases produced by neutron irradiation. Chemical Geology, 437: 77-87.

Scaillet, B. and Evans, B.W., 1999. The 15 June 1991 Eruption of Mount Pinatubo. I. Phase Equilibria and Pre-eruption P-T-fO_2-fH_2O Conditions of the Dacite Magma. Journal of Petrology, 40(3): 381-411.

Schiavi, F. et al., 2015. Geochemical heterogeneities in magma beneath Mount Etna recorded by 2001–2006 melt inclusions. Geochemistry, Geophysics, Geosystems, 16(7): 2109-2126.

Sekimoto, S. and Ebihara, M., 2016. Accurate Determination of Chlorine, Bromine and Iodine in U.S. Geological Survey Geochemical Reference Materials by Radiochemical Neutron Activation Analysis. Geostandards and Geoanalytical Research: doi:10.1111/ggr.12145.

Seo, J.H., Guillong, M., Aerts, M., Zajacz, Z. and Heinrich, C.A., 2011. Microanalysis of S, Cl, and Br in fluid inclusions by LA-ICP-MS. Chem. Geol., 284(1-2): 35-44.

Shimizu N., Semet M.P., Allegre C.J., 1978. Geochemical applications of quantitative ion-microprobe analysis. Geochimica et Cosmochimica acta, 42, 1321-1334.

Shishkina, T.A., Botcharnikov, R.E., Holtz, F., Almeev, R.R. and Portnyagin, M.V., 2010. Solubility of H_2O- and CO_2-bearing fluids in tholeiitic basalts at pressures up to 500 MPa. Chemical Geology, 277(1-2): 115-125.

Solé, V.A., Papillon, E., Cotte, M., Walter, P. and Susini, J., 2007. A multiplatform code for the analysis of energy-dispersive X-ray fluorescence spectra. Spectrochim. Acta Part B, 62: 63–68.

Theys, N. et al., 2009. First satellite detection of volcanic bromine monoxide emission after the Kasatochi eruption. Geophys. Res. Lett., 36: L03809.

Figure Captions

Figure 1. Br contents (ppm) measured by INAA in the silicate glasses of basaltic, andesitic and rhyodacitic compositions, as a function of the nominal Br content (the amount of Br loaded into the experimental charges). Both the calculated uncertainty for the nominal contents (between 1.9 and 5.5 %) and the standard deviation for the value measured by INAA are smaller than the symbols. **(a)** all analysed standards; **(b)** a blow-up showing the low Br concentration range.

Figure 2. Mean blank-corrected peak areas of SR-XRF measurements versus Br nominal contents in basaltic glasses. Each point represents the average of 4 analyses, the error bar shows the standard deviation. **(a)** all analysed standards, **(b)** standards with Br contents ≤ 12 ppm.

Figure 3. ^{79}Br (cps)/ ^{24}Mg (cps) ratios measured by LA-ICP-MS versus Br nominal contents in basaltic, andesitic and rhyolitic glasses. Each point represents a single analysis. Note the different slope of the regression line for rhyodacite with respect to those of andesite and basalt. **(a)** all analysed standards. **(b)** standards with Br contents ≤ 1100 ppm.

Figure 4. Plots of calculated Br (ppm)/SiO_2 (wt%) ratio versus measured ^{79}Br/$^{28}SiO_3$ ratio of basaltic, andesitic and rhyodacitic glasses with the SIMS. On the log-log plot **(a)**, the data show a linear relationship over several orders of magnitude, indicating the absence of instrumental saturation or instrumental background. On the normal linear plot **(b)**, the basaltic glasses and the rhyodacitic glasses define distinct regression lines.

Figure 5. Br contents (ppm) quantified using the three different techniques (LA-ICP-MS, SIMS, SR-XRF) versus Br nominal contents in the standard glasses. Each point represents the average of several analyses, and the error bar shows the standard deviation. **(a)** all analysed standards. **(b)** standards with Br contents ≤ 100 ppm. **(c)** analytical accuracy calculated for every sample as a function of its Br nominal content, for the three methods. The accuracy is estimated by computing the relative difference between the mean Br content and the nominal value (Table 3).

Table 1. Composition of the starting whole-rocks and their corresponding dry glasses used to synthesize the Br standard glasses

	Etna 11/22/2002 eruption (ET02PA27)		**Santorini USC-2 eruption (S09-22)**		**Santorini Minoan eruption (S82-30)**	
	Whole-rock[a]	Dry glass[b]	Whole-rock[c]	Dry glass[c]	Whole-rock[d]	Dry glass[d]
Major oxides (wt%)		*n = 32*		*n = 8*		*n = 22*
SiO_2	47.64	47.95 (82)	59.87	58.88 (43)	70.58	71.24 (26)
TiO_2	1.71	1.67 (11)	1.16	1.28 (5)	0.46	0.45 (4)
Al_2O_3	16.6	17.32 (27)	15.84	16.16 (17)	14.64	14.87 (15)
Fe_2O_{3tot}	11.52	10.24* (13)	8.46	8.18* (25)	3.05	2.85* (18)
MnO	0.18	0.17	0.17	0.20 (9)	0.08	0.08 (5)
MgO	6.14	5.72 (28)	2.39	2.77 (9)	0.66	0.73 (5)
CaO	10.56	10.85 (37)	5.70	6.46 (12)	2.36	2.34 (14)
Na_2O	3.51	3.42 (16)	4.39	4.07 (15)	5.08	4.24 (8)
K_2O	1.99	1.98 (10)	1.79	1.67 (6)	3.00	3.08 (11)
P_2O_5	0.54	0.51 (12)	0.24	0.31 (6)	0.08	0.13 (4)
Rare Earth Elements (ppm)						
La	49.90		19.31	17.26	30	26.57
Ce	101.00		42.18	37.20	40	53.71
Pr	12.00		5.30		n.a.	
Nd	48.10		22.15	19.44	n.a.	21.87
Pm	n.a.		n.a.		n.a.	
Sm	8.90		5.63		n.a.	
Eu	2.67		1.47		n.a.	
Gd	8.30		6.18		n.a.	
Tb	1.04		1.05		n.a.	
Dy	5.56		6.69		n.a.	

Ho	1.01	1.42	n.a.
Er	2.58	4.22	n.a.
Tm	0.35	0.65	n.a.
Yb	2.19	4.51	n.a.
Lu	0.32	0.72	n.a.
Total REE	243.91	121.49	
Total LREE	230.87	102.22	

Major elements analyses are recalculated to 100%
a: sample provided by N. Métrich. Whole-rock composition from Schiavi et al. (2015), XRF and ICP-MS data.
b: from Iacono-Marziano et al. (2012), EMP data.
c: this study (whole-rock analysed by ICP-OES at SARM-CRPG, France; dry glass analysed with a Cameca SX50 EMP, BRGM-ISTO, Orléans, France. REE contents of dry glass determined by LA-ICP-MS at LMV, Clermont-Ferrand)
d: Cadoux et al. (2014) and La, Ce, Nd contents determined by LA-ICP-MS (LMV, Clermont-Ferrand)
n: number of analyses; numbers in brackets are standard deviations in terms of least unit cited
n.a.: not analysed
* FeO_{tot} : total Fe as FeO

Table 2. Major elements composition (in wt%) of the basaltic, andesitic and rhyodacitic standard glasses

	Basalts																			
Sample name	B0.5		B1		B5		B10		B50		B100		B300		B600		B1000		B3000		B6000	
Loaded Br (ppm)	0.5		1		5		12		52		100		294		593		967		2694		5968	
Capsule metal	Pt		Pt		Pt		Pt		Au-Pd		Au-Pd		Au-Pd		Au-Pd		Au-Pd		Au-Pd		Au-Pd	
	n = 5	*SD*	*n = 5*	*SD*	*n = 9*	*SD*	*n = 5*	*SD*	*n = 15*	*SD*	*n = 15*	*SD*	*n = 15*	*SD*	*n = 15*	*SD*	*n = 15*	*SD*	*n = 15*	*SD*	*n = 15*	*SD*
SiO_2 (wt.%)*	45.57	0.27	46.25	0.31	45.68	0.45	45.85	0.47	45.86	0.24	44.69	0.33	46.75	0.34	46.49	0.45	45.62	0.28	47.01	0.42	45.22	0.48
TiO_2	1.57	0.02	1.63	0.07	1.67	0.04	1.61	0.02	1.65	0.02	1.60	0.02	1.62	0.08	1.65	0.09	1.66	0.08	1.64	0.08	1.67	0.10
Al_2O_3	15.67	0.16	15.70	0.32	15.48	0.38	15.53	0.31	15.36	0.16	15.01	0.19	15.32	0.29	15.42	0.21	15.32	0.20	15.66	0.18	15.56	0.18
FeOtot	9.82	0.16	10.16	0.22	9.86	0.56	9.86	0.20	9.44	0.17	9.38	0.18	9.21	0.13	9.17	0.13	9.77	0.11	8.99	0.19	9.56	0.10
MnO	0.18	0.03	0.12	0.07	0.19	0.01	0.13	0.09	0.17	0.09	0.17	0.02	0.19	0.00	0.17	0.03	0.13	0.02	0.18	0.00	0.16	0.02
MgO	6.19	0.06	6.16	0.07	6.25	0.14	6.21	0.07	6.08	0.04	6.02	0.04	5.97	0.06	6.00	0.02	6.17	0.02	5.95	0.03	6.18	0.03
CaO	10.13	0.16	10.04	0.09	10.13	0.11	10.19	0.17	10.04	0.09	9.71	0.09	9.94	0.09	9.84	0.08	9.97	0.07	9.90	0.04	9.92	0.06
Na_2O	3.13	0.07	3.04	0.08	3.05	0.09	3.11	0.05	3.10	0.09	2.99	0.02	2.99	0.00	3.03	0.01	3.13	0.01	3.22	0.01	3.42	0.02
K_2O	0.46	0.25	0.50	0.26	0.55	0.22	0.47	0.28	1.87	0.07	1.81	0.08	1.84	0.06	1.88	0.08	1.83	0.09	1.93	0.09	1.87	0.08

P_2O_5	1.80	0.11	1.88	0.1	1.87	0.1	1.90	0.23	0.75	0.10	0.70	0.07	0.68	0.06	0.72	0.09	0.74	0.09	0.73	0.08	0.72	0.08
Sum	94.52		95.49		94.73		94.85		94.42		92.25		94.62		94.53		94.42		95.33		94.36	
H_2O (wt.%)**					2.04		2.11						2.06						2.07		1.50	

Table 2. continued

	Andesites										Rhyodacites									
Sample name	A10		A50		A100		A500		A1000		RD10		RD50		RD1000		RD5000		RD10000	
Loaded Br (ppm)	10		50		99		497		1081		10		52		100		478		5350	
Capsule metal	Pt		Pt		Pt		Pt		Pt		Pt		Pt		Pt		Pt		Pt	
	n = 6	*SD*	*n = 7*	*SD*	*n = 5*	*SD*	*n = 5*	*SD*	*n = 6*	*SD*	*n = 10*	*SD*	*n = 6*	*SD*	*n = 7*	*SD*	*n = 7*	*SD*	*n = 6*	*SD*
SiO_2 (wt.%)*	57.52	0.51	55.94	0.74	56.70	0.57	56.97	0.25	55.58	0.22	67.11	0.53	67.77	0.47	67.55	0.33	67.14	0.62	67.66	0.34
TiO_2	1.28	0.09	1.13	0.07	1.06	0.03	1.22	0.07	1.14	0.03	0.35	0.03	0.39	0.08	0.35	0.05	0.39	0.04	0.34	0.02
Al_2O_3	15.59	0.26	15.12	0.23	15.31	0.19	15.43	0.20	15.26	0.09	13.71	0.20	14.07	0.20	13.94	0.18	13.82	0.27	14.18	0.10
		0.36		0.44		0.20		0.20		0.30		0.54		0.30		0.25		0.15		0.16
FeOtot	5.725		5.994		6.766		5.379		6.198		2.884		2.970		2.472		2.563		*0.866*	
MnO	0.16	0.11	0.23	0.11	0.22	0.00	0.14	0.11	0.24	0.11	0.07	0.00	0.11	0.00	0.10	0.11	0.13	0.00	0.09	0.00

		0		0		9		1		1		9		6		1		9		7
		0.0		0.0		0.0		0.0		0.0		0.0		0.0		0.0		0.0		0.0
MgO	2.60	5	2.58	7	2.74	6	2.74	5	2.60	3	0.65	4	0.67	5	0.67	4	0.69	4	0.66	4
		0.0		0.1		0.0		0.1		0.1		0.1		0.0		0.0		0.0		0.1
CaO	6.00	8	5.98	7	6.18	9	6.22	1	6.08	3	2.30	1	2.24	8	2.27	7	2.28	5	2.32	4
		0.1		0.1		0.0		0.0		0.0		0.1		0.0		0.1		0.1		0.0
Na_2O	4.15	4	4.25	2	4.01	3	4.21	7	4.33	8	4.65	0	4.55	5	4.52	0	4.56	1	4.72	9
		0.1		0.1		0.1		0.0		0.0		0.1		0.0		0.1		0.1		0.0
K_2O	1.66	5	1.68	6	1.55	0	1.68	7	1.60	5	3.03	4	3.02	6	2.99	3	2.91	6	2.97	9
		0.2		0.0		0.1		0.1		0.0		0.1		0.0		0.0		0.1		0.0
P_2O_5	0.25	2	0.22	8	0.23	7	0.29	5	0.25	7	0.08	0	0.08	8	0.07	6	0.12	5	0.07	7
	94.9		93.1		94.7		94.2				94.8		95.8							
Sum	4		1		6		7		93.26		5		7		94.92		94.60		93.87	
H_2O (wt.%)**	4.98		4.48		4.90		6.45		5.98		4.21		3.85		4.17		4.75		4.20	

* Major elements composition determined by electron microprobe (average of at least 5 spot analyses)
** H_2O content (average of 3 to 6 analyses) measured by SIMS (IMS 1280, CRPG, Nancy, France)
RD5000 displays anomalously low FeO: this is due to a longer run duration (following technical problems) which favored alloy of Fe with Pt from the capsule

Table 3. Bromine contents (ppm) in the standard glasses as determined by the different analytical methods

Sample name	Loaded amounts of Br	error * (%)	Br contents measured by INAA	INAA /loaded Br contents	Br contents measured by techniques needing calibration		
					SR-XRF	LA-ICP-MS	SIMS
RD10	10.13	2.7	8.90 (3)	0.88	n.a.	n.a.	3.9 (1)
RD50	51.8	2.1	51.00 (7)	0.98	n.a.	n.a.	18 (1)
RD100	100	2.2	104.0 (5)	1.04	n.a.	119	139 (4)
RD500	478	2.2	496.0 (1.4)	1.04	n.a.	483 (8)	580 (23)
RD5000	5350	2.0	5030.0 (8.7)	0.94	n.a.	5355 (635)	5638 (310)
A10	10.1	2.7	9.9 (2)	0.98	n.a.	n.a.	16.2 (1.2)
A50	49.7	2.2	51.3 (1.0)	1.03	n.a.	n.a.	83.3 (5)
A100	99	2.2	90.3 (3)	0.91	n.a.	136	136 (7)
A500	497	2.1	524.0 (1.6)	1.05	n.a.	423 (11)	381 (20)
A1000	1081	1.9	990.0 (3.2)	0.92	n.a.	1102 (192)	1127 (48)
B0.5	0.5	4.5	54	108.00	0.8 (2)	n.a.	n.a.
B1	1	3.6	105	105.00	1.4 (4)	n.a.	3.5 (5)
B5	5		182	36.40	4 (1)	n.a.	3.7 (8)
B10	12	5.5	40	3.33	13 (3)	n.a.	6.5 (5)
B50	52	5.1	83	1.60	53 (5)	n.a.	n.a.
B100	100	5.2	118	1.18	97 (10)	n.a.	n.a.
B300	294	5.2	305	1.04	n.a.	264 (12)	n.a.
B600	593	5.0	634	1.07	n.a.	508 (11)	n.a.
B1000	967	5.0	1280	1.32	1060 (106)	1064 (118)	n.a.
B3000	2694	5.1	3240	1.20	2747 (274)	2740 (516)	3034 (47)
B6000	5968	3.5	6930	1.16	5683 (568)	5670 (102)	5755 (37)

RD: rhyodacite, A: andesite, B: basalt
* error on the calculated bromine contents in the experimental charges taking in to account the errors on the successive weighings of
NaBr salt, H_2O, glass powder and H_2O-NaBr
solution
INAA results are from University of Massachusetts Radiation Laboratory (USA) for RD and A, and from Actlabs (Canada) for B.

n.a.: not analysed

Numbers in brackets are standard deviations in terms of least unit cited (based on replicate counts for INAA).

Number of analyses per sample: 4 for SR-XRF, 3-10 for LA-ICP-MS, 3-6 for SIMS.

Table 4. SIMS measurements in MPI-DING glasses

	SiO2 (wt%)*	Br (ppm)*	background (mass 78.8) signal (cps)	^{79}Br signal (cps)	^{81}Br signal (cps)	^{81}Br /^{79}Br	error	^{79}Br /$^{28}SiO_3$	error	Calculated Br (ppm)**
ATHO-G	75.6	1.2	0.02	214.38	209.55	0.97834	0.01033	0.0000236	0.0000004	1.04
			0.08	199.08	194.75	0.98527	0.00491	0.0000219	0.0000003	0.97
			0.03	202.87	194.34	0.96879	0.00661	0.0000225	0.0000003	0.99
			0.06	204.41	200.15	0.99264	0.00797	0.0000230	0.0000003	1.02
			0.03	209.50	202.77	0.98839	0.01076	0.0000234	0.0000003	1.03
			0.03	209.62	202.23	0.97013	0.00764	0.0000234	0.0000003	1.03
			0.02	205.63	198.71	0.97495	0.00733	0.0000230	0.0000003	1.01
			0.06	209.68	201.77	0.97780	0.00643	0.0000229	0.0000003	1.01
			0.05	197.61	188.73	0.95127	0.01132	0.0000224	0.0000005	0.99
			0.00	203.43	197.71	0.97772	0.01158	0.0000227	0.0000004	1.00
Average								***0.0000229***		***1.01***
Standard deviation								***0.0000005***		***0.02***
Uncertainty at 95% confidence level								***1.41%***		
StHs6/80-G	63.7	0.8	0.02	207.52	187.77	0.90880	0.00949	0.0000318	0.0000005	0.93
			0.02	191.20	177.16	0.94203	0.00667	0.0000304	0.0000005	0.89
			0.02	208.59	189.41	0.91291	0.00827	0.0000327	0.0000006	0.95
			0.05	206.20	185.67	0.90521	0.01383	0.0000328	0.0000006	0.95
			0.06	199.66	191.09	0.96271	0.01043	0.0000313	0.0000005	0.91
			0.00	206.15	190.41	0.93242	0.00831	0.0000328	0.0000006	0.96
			0.03	204.25	194.80	0.97286	0.00850	0.0000327	0.0000007	0.95
			0.06	218.23	192.10	0.88597	0.00732	0.0000359	0.0000004	1.05
			0.02	210.97	186.36	0.89224	0.01218	0.0000347	0.0000006	1.01

Average	***0.0000328***	***0.95***
Standard deviation	***0.0000017***	***0.05***
Uncertainty at 95% confidence level	***3.37%***	

* values from Jochum et al. (2006)

** calculated from regression curves built with the rhyodacitic and andesitic standards presented in this study

Figure 1

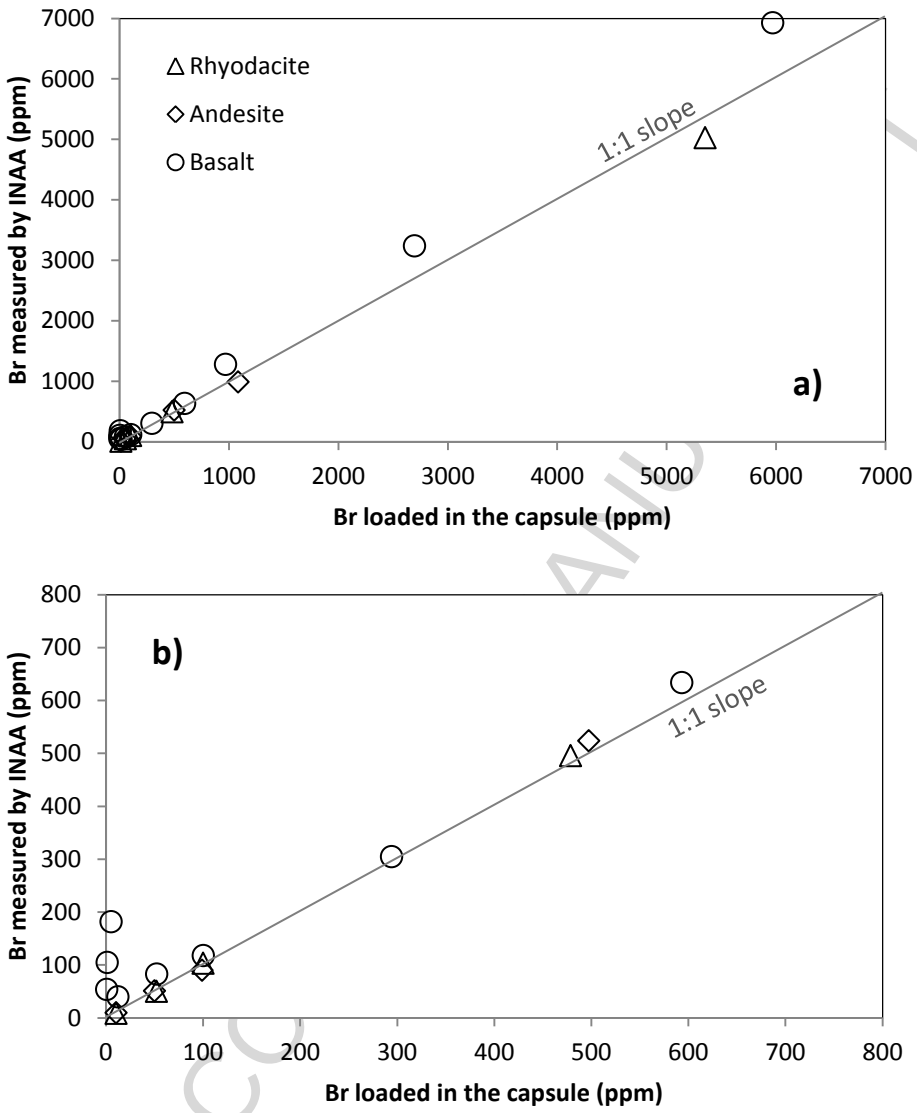

Figure 2

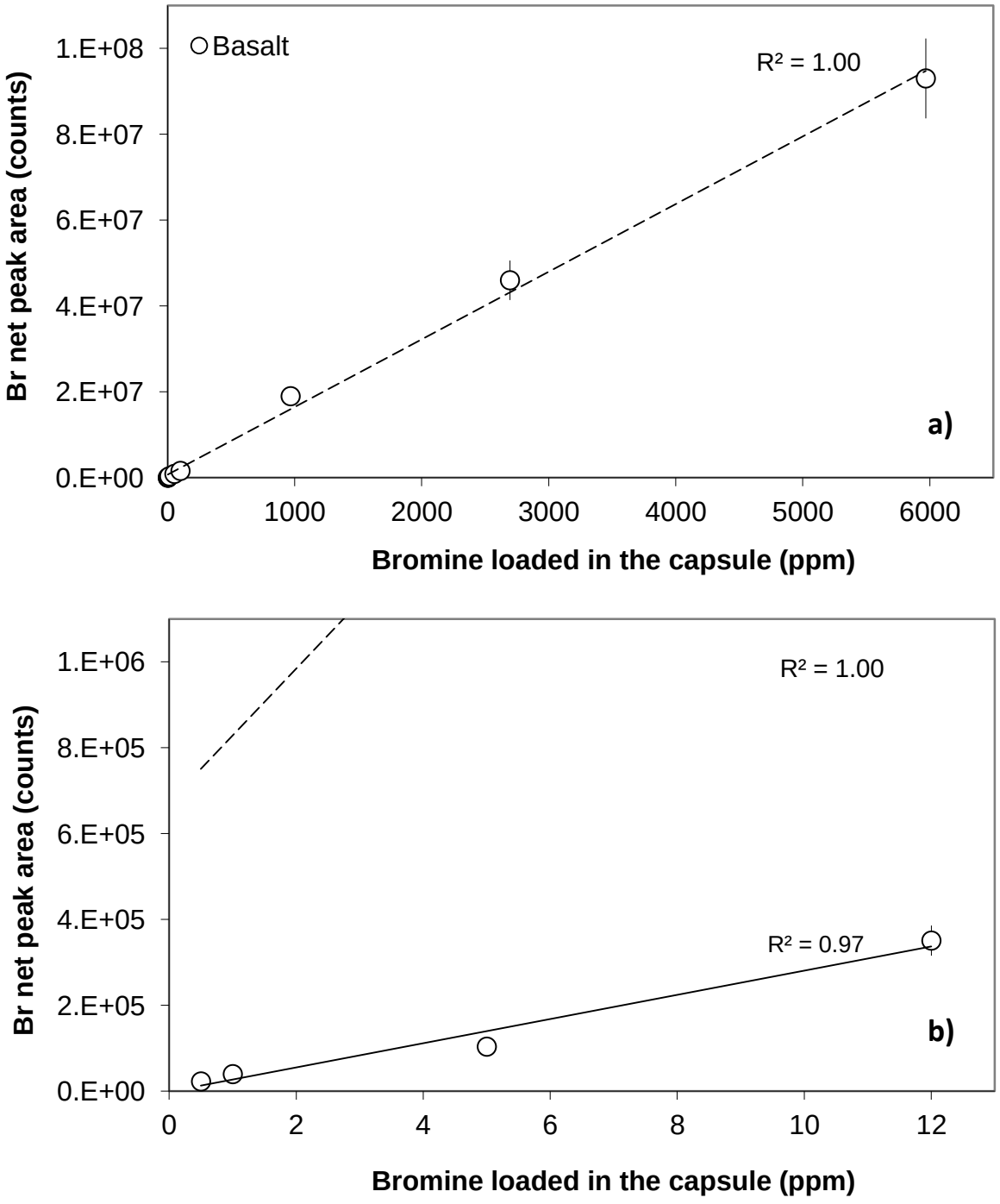

Figure 3

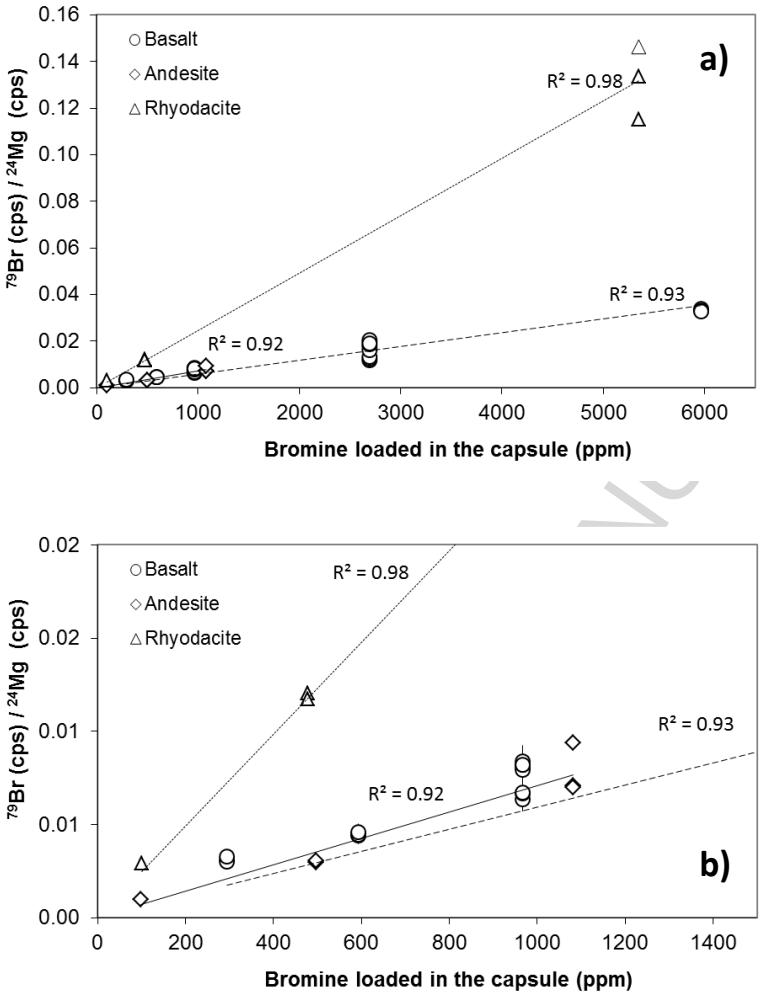

Figure 4

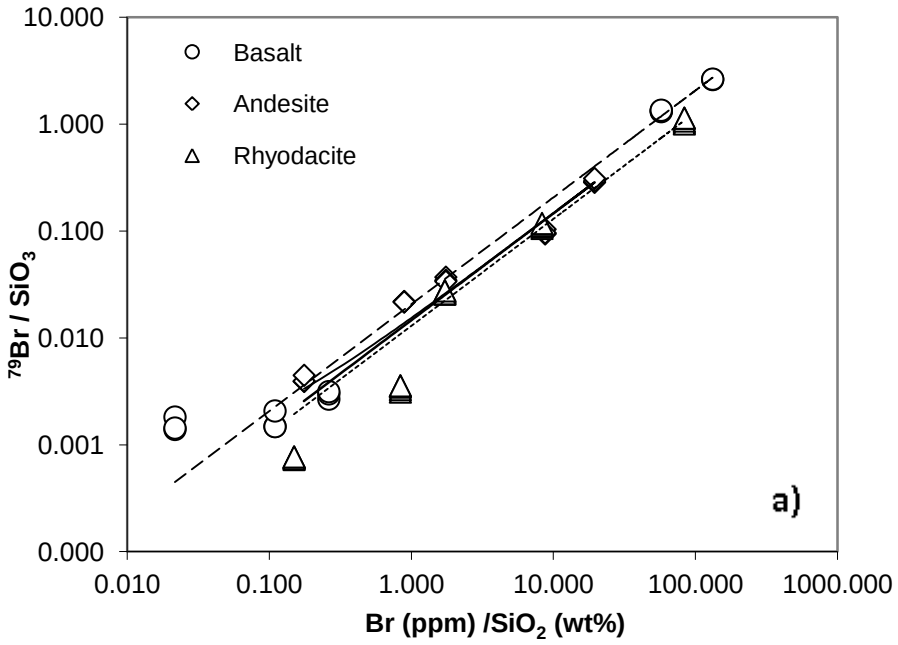

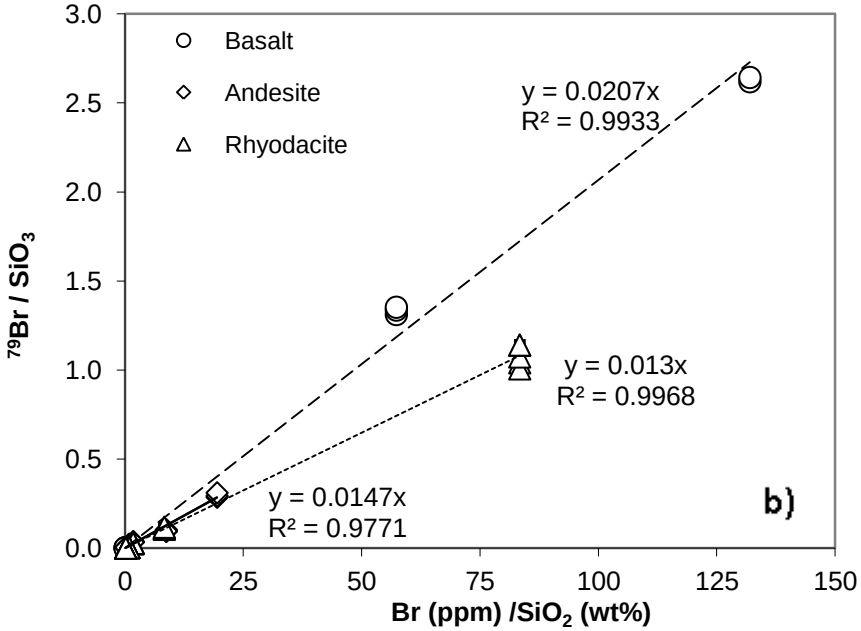

Figure 5